研究成果の刊行物・別刷り

In utero exposure to dioxin causes neocortical dysgenesis through the actions of $p27^{Kip1}$

Takayuki Mitsuhashi[a], Junzo Yonemoto[b], Hideko Sone[b], Yasuhiro Kosuge[a,1], Kenjiro Kosaki[a], and Takao Takahashi[a,2]

[a]Department of Pediatrics, School of Medicine, Keio University, Shinjuku-ku, Tokyo 160-8582, Japan; and [b]Research Center for Environmental Risk, National Institute for Environmental Studies, Tsukuba-City, Ibaraki 305-8506, Japan

Edited by Pasko Rakic, Yale University, New Haven, CT, and approved July 13, 2010 (received for review March 8, 2010)

Dioxins have been reported to exert various adverse effects, including cell-cycle dysregulation in vitro and impairment of spatial learning and memory after in utero exposure in rodents. Furthermore, children born to mothers who are exposed to dioxin analogs polychlorinated dibenzofurans or polychlorinated biphenyls have developmental impairments in cognitive functions. Here, we show that in utero exposure to dioxins in mice alters differentiation patterns of neural progenitors and leads to decreased numbers of non-GABAergic neurons and thinner deep neocortical layers. This reduction in number of non-GABAergic neurons is assumed to be caused by accumulation of cyclin-dependent kinase inhibitor $p27^{Kip1}$ in nuclei of neural progenitors. Lending support to this presumption, mice lacking $p27^{Kip1}$ are not susceptible to in utero dioxin exposure. These results show that environmental pollutants may affect neocortical histogenesis through alterations of functions of specific gene(s)/protein(s) (in our case, dioxins), exerting adverse effects by altering functions of $p27^{Kip1}$.

environmental pollutants | cerebral cortex | development | neuronal progenitor cells | cell cycle

Dioxins are ubiquitous environmental pollutants that have been known to disturb hormonal homeostasis in mammals (1–3). In utero exposure to 2,3,7,8-tetrachlorodibenzo-*p*-dioxin (TCDD), one of the most potent dioxins, has been shown to cause impaired spatial learning and memory in rats (4). Furthermore, in humans, it is reported that children born to mothers who are exposed to dioxin analogs polychlorinated dibenzofurans (PCDFs) or polychlorinated biphenyls (PCBs) have developmental impairments in higher cognitive functions (2, 5). Additionally, a recent report describes the relationship between prenatal exposure level of polycyclic aromatic hydrocarbons and child intelligence at 5 y of age (6). However, the mechanisms by which dioxin exposure in utero affects the higher cortical functions after birth remain undetermined.

Non-GABAergic projection neurons, accounting for 80% of the neocortical neurons, are produced by proliferation/differentiation of neuronal progenitor cells (NPCs) constituting the pseudostratified ventricular epithelium [PVE; roughly coexistent with the ventricular zone (VZ)] along the lateral ventricular surface of the embryonic forebrain. The term PVE has been adopted, because it excludes postmitotic, premigratory neuroblasts of the subventricular zone (7, 8). In mice, the NPCs undergo 11 cell divisions during the period of neocortical histogenesis, with the length of the cell cycle (T_C) increasing by 2-fold from 8 to 18 h, mainly because of prolongation of the G1 phase of the cell cycle (T_{G1}) (8). During the same period, the proportion of daughter cells that become postmitotic during each cell cycle [quiescent (Q) fraction] increases (9). It is of critical importance that the layer position of the non-GABAergic projection neurons is strongly correlated with the cell cycle of origin (that is, the cell cycle at which a given non-GABAergic neuron becomes mitotically quiescent and starts radial migration to the neocortex) (10). Taken together, the regulated patterns of increase of the T_{G1} and Q fractions and strict correlation between the layer position and the cell cycle of origin both strongly suggest a link between cell-cycle regulation of the G1 phase and neuronal cell-class determination (layer destination of projection neurons) (10).

Progression of the cell cycle is precisely controlled by a set of proteins including cyclins, cyclin dependent kinases (CDKs), and CDK inhibitors (11). $p27^{Kip1}$, one of the CDK inhibitors, specifically inhibits the activity of cyclin E/CDK2 kinase and inhibits entry of the cells into the S phase (12, 13). Indeed, some of the critical events during the G1 phase of the cell cycle in NPCs are regulated by $p27^{Kip1}$: alterations in $p27^{Kip1}$ expression in the NPCs result in changes in the Q fraction, thereby altering the number of neurons to be produced and hence, the thickness of the neocortex. Specifically, overexpression of $p27^{Kip1}$ in NPCs in vivo increases the Q fraction (that is, promotes differentiation of the NPCs), with a resultant thinner neocortex (14, 15), whereas the lack of $p27^{Kip1}$ decreases the Q fraction, resulting in a thicker neocortex (16). It is worthy of note in this context that TCDD has been reported to induce $p27^{Kip1}$ and delay the G1 phase of the cell cycle in a hepatoma cell line, fetal thymocytes, and human neuronal cell line (17). Taken together, these observations suggest that in utero exposure to TCDD is likely to alter the proliferative behaviors of the NPCs by inducing $p27^{Kip1}$ protein expression, resulting in abnormalities of neocortical histogenesis.

Here, we report that in utero exposure to TCDD indeed modified the $p27^{Kip1}$ activities in NPCs to cause neocortical dysgenesis. These observations can be explained by a hypothetical mathematical model where both the increase in Q fraction and the neuronal class switch occur prematurely compared with that under physiological conditions.

Results

TCDD Exposure in Utero Reduced the Size of the Telencephalon and Thickness of the Neocortex as Assessed on Postnatal Day 21. The telencephalon, olfactory bulb, and cerebellum of TCDD-treated mice showed a normal appearance on postnatal day (P) 21 (Fig. 1*A*). However, the forebrains in these TCDD-treated animals were smaller, with the width and length being reduced by 4.78% (9.48 ± 0.063 mm vs. 9.93 ± 0.030 mm in the controls; $P < 0.001$, $n = 10$) and 2.29% (8.37 ± 0.048 vs. 8.57 ± 0.035 mm; $P = 0.004$, $n = 10$), respectively, compared with the values in the controls. The reductions in the width and length of the telencephalon indicate that TCDD exposure in utero caused roughly 7% reduction of the neocortical surface area. The thickness of the primary somatosensory cortex was reduced by 14.9% (750 ± 29.2 vs. 881.3 ± 13.2 μm; $P < 0.001$, $n = 6$) (Fig. 1*B*); the thickness of the deeper

Author contributions: T.M., J.Y., H.S., K.K., and T.T. designed research; T.M. and Y.K. performed research; T.M. and T.T. analyzed data; and T.M. and T.T. wrote the paper.

The authors declare no conflict of interest.

This article is a PNAS Direct Submission.

Freely available online through the PNAS open access option.

[1]Present address: Research Unit of Pharmacology, School of Pharmacy, Nihon University, Chiba 274-8555, Japan.

[2]To whom correspondence should be addressed. E-mail: ttakahashi@z3.keio.jp.

This article contains supporting information online at www.pnas.org/lookup/suppl/doi:10.1073/pnas.1002960107/-/DCSupplemental.

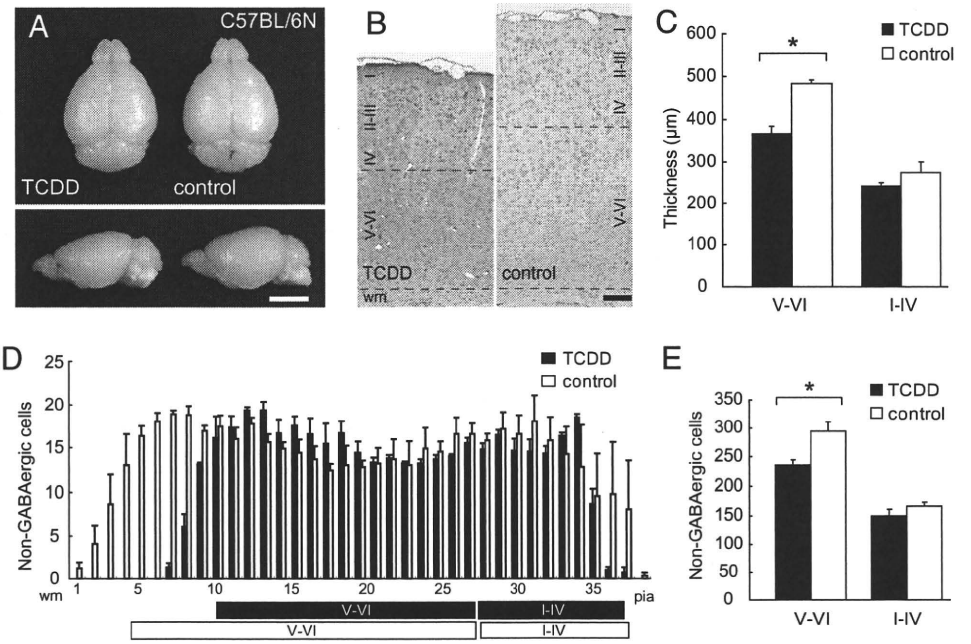

Fig. 1. Effects of in utero TCDD exposure observed on postnatal day 21. (*A*) Macroscopic dorsal and lateral overview of the whole brain from TCDD-treated and control C57BL/6N mice. (Scale bar, 5 mm.) (*B*) High-power view of the primary somatosensory neocortex of the TCDD-treated and control mice. Brown cells, GABA-positive interneurons; purple nuclei, either non-GABAergic projection neurons or glial cells; black dotted lines, boundaries between layers I-IV/V-VI and gray matter/white matter (wm). (Scale bar, 100 μm.) (*C*) Thickness of layers V-VI and I-IV in the TCDD-treated and control mice shown in *B*. (*D*) Numbers of non-GABAergic neurons counted in each bin (250 μm in width and 25 μm in height) lined serially from wm to the pial surface (pia) in the primary somatosensory neocortex shown in *B*. Black and white boxes under the abscissa indicate layers I-IV/V-VI in the neocortex of the TCDD-treated and control mice, respectively. (*E*) Total number of non-GABAergic neurons in layers V-VI and I-IV. $*P < 0.05$. Error bars in *C–E*, SEM.

cortical layers (layers V-VI) was reduced by 24.1% (366.7 ± 16.67 vs. 483.3 ± 8.33 μm; $P = 0.005$, $n = 6$), whereas no significant change in the thickness of the superficial layers (layers I-IV) was noted (241.7 ± 8.33 vs. 275.0 ± 25.0 μm; $P = 0.38$, $n = 6$) (Fig. 1*C*).

TCDD Exposure in Utero Reduced the Number of Non-GABAergic Neurons in the Deeper Cortical Layers as Assessed on Postnatal Day 21. We identified non-GABAergic projection neurons by the lack of positive immunohistochemical staining of the cells with anti-GABA antibody (Fig. 1 *B* and *D*). The number of non-GABAergic projection neurons in the primary somatosensory neocortex on P21 was significantly reduced in the deeper layers of the TCDD-treated animals by 20.0% compared with that in normal controls (Fig. 1*E*) (235.6 ± 9.24 vs. 294.3 ± 16.9 per 1,000 μm^2; $P = 0.037$, $n = 3$). However, there was no significant difference in the number of non-GABAergic neurons in the superficial layers of the cortex in the TCDD-treated animals compared with that in the controls (Fig. 1*E*) (149.8 ± 10.9 vs. 166.8 ± 6.14 per 1,000 μm^2; $P = 0.246$, $n = 3$). No alteration in the cell-packing density of the non-GABAergic projection neurons was observed in either the deeper or superficial layers in the TCDD-treated animals. Taken together, we concluded that the reduction in neocortical thickness of the TCDD-treated mice was caused by the reduction in the number of non-GABAergic projection neurons in the deeper cortical layers.

Total Cell Cycle Length of the NPCs Was Not Altered by TCDD Exposure in Utero. Next, we examined the TCDD-treated embryonic forebrains on E12, the time point at which the non-GABAergic neurons of the deeper layers (layers V–VI) are to be produced (10). Histologically, the dorsomedial cerebral wall, the future primary somatosensory neocortex, was normal in the TCDD-treated embryos (Fig. 2*A*). The S phase zone, where accumulation of the nuclei of the NPCs is observed during the S phase of the cell cycle, in the dorsomedial cerebral wall was located between 60 and 70 μm from the lateral ventricular border on E12 in the TCDD-treated mice, similar to the finding in the normal control mice (Fig. 2 *A* and *B*) ($n = 4$). At 4 h after exposure to bromodeoxyuridine (BrdU), BrdU-positive nuclei moved to the ventricular surface in both the TCDD-treated and control animals, indicating that the interkinetic nuclear migration in the embryonic forebrain operated normally in the TCDD-treated mice (Fig. 2*C*) ($n = 3$). After 6.5 h exposure to BrdU, virtually all of the nuclei in the VZ were BrdU-positive in both the TCDD-treated and control mice, indicating that the growth fractions in the VZ were nearly equal to 1.0 in both the TCDD-treated and control mice (Fig. 2*D*) ($n = 3$). The results of cumulative BrdU labeling (Fig. 2*E*) (18) revealed that the total cell-cycle length of the NPCs in the forebrain of the TCDD-treated animals was 10.7 h, not significantly different from that in the controls (Table 1).

TCDD Exposure in Utero Promoted Early Cell Cycle Exit of NPCs. We then identified the NPCs in the Q fraction and P fraction (the fraction of daughter cells that remain proliferative; $P = 1.0 - Q$) on E12 by using two S-phase tracers, iododeoxyuridine (IdU) and BrdU (Fig. 2*F*) (15, 19). In the dorsomedial cerebral wall of the TCDD-treated mice, the IdU-positive nuclei (blue nuclei) were located in the outer margin of the S-phase zone in both the P + Q and Q experiments (Fig. 2*F*). The distribution patterns of the P + Q and Q cells were not different between the TCDD-treated and control animals (Fig. 2*G*). An increase in the number of Q cells was observed in the TCDD-treated animals, with an estimated Q fraction of 0.17, which represented a 21.4% increase compared with the value in the controls (Table 2) ($n = 3$).

TCDD Exposure in Utero Increased the Nuclear Fraction of the p27^{Kip1} Protein in the NPCs. To elucidate the molecular mechanisms underlying the aforementioned changes, we first investigated the TCDD-induced changes in the mRNA expression levels of cell-cycle regulatory genes in the dorsomedial cerebral wall by dot blot hybridization (Fig. 3 *A* and *B*) ($n = 5$). We observed up-regulation

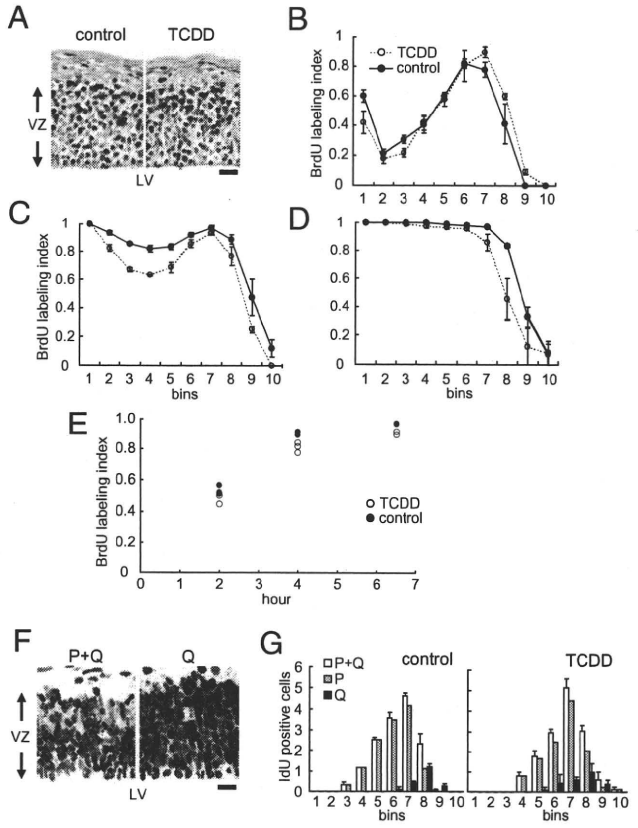

Fig. 2. Effects of in utero TCDD exposure on the cell-cycle kinetics of the NPCs. (*A*) High-power views of the dorsomedial cerebral wall of the E12 forebrains of the control and TCDD-treated mice. Black, BrdU-labeled nuclei; red, non–BrdU-labeled nuclei; VZ, ventricular zone; LV, lateral ventricle. (Scale bar, 10 μm.) (*B*) The 2-h BrdU-labeling index was evaluated in each bin (100 μm in width and 10 μm in height) lined serially from the lateral ventricle to the pial surface in the ventricular zone. The 4-h (*C*) and 6.5-h (*D*) BrdU-labeling indices are also shown. (*E*) Total labeling indices after cumulative BrdU exposure. (*F*) High-power views of the dorsomedial area of the E12 forebrains of mice exposed to TCDD. Blue nuclei, IdU-only positive; brown nuclei, double positive for IdU and BrdU. In the P + Q experiment (*Left*), blue nuclei correspond to the P + Q fraction cells. In the Q experiment (*Right*), blue cells correspond to only the Q fraction cells. (Scale bar, 10 μm.) (*G*) The number of Q fraction cells and P + Q fraction cells that were counted in each bin in control (*Left*) and TCDD-treated embryos (*Right*).

of the *p27*^{Kip1} and *p15*^{INK4b} mRNAs in the E12 forebrain in the TCDD-treated animals compared with the expressions in the controls (Fig. 3*B*): both *p27*^{Kip1} and *p15*^{INK4b} are CDK inhibitors that are known to promote exit from the cell cycle (11). We then analyzed the p27^{Kip1} and p15^{INK4b} protein levels by immunoblot analysis of lysates of the E12 dorsomedial cerebral walls. The p27^{Kip1} and p15^{INK4b} protein levels in the total tissue lysate were not significantly different between the TCDD-treated and control animals. However, when only the nuclear fractions from the dorsomedial cerebral wall were analyzed, the p27^{Kip1} protein level was

Table 1. Lengths of each phase of the cell cycle estimated by cumulative BrdU labeling index

	$T_C - T_S$	T_C	T_S	T_{G1}	T_{G2+M}
TCDD	7.0	10.7	3.7	5.0	2.0
Control	6.3	10.5	4.3	4.3	2.0

T_C, length of the total cell cycle; T_S, length of S phase, T_{G1}, length of G1 phase; T_{G2+M}, length of G2 + M phase.

Table 2. Q fraction analysis

	N_{P+Q}	N_Q	P fraction	Q fraction
TCDD	14.5	2.6	0.82	0.17
Control	14.7	2.1	0.86	0.14

N_{P+Q}, number of blue nuclei in the P + Q experiment; N_Q, number of blue nuclei in the Q experiment; Q fraction, N_Q/N_{P+Q}; P fraction, 1 − Q.

about 2.5-fold higher in the TCDD-treated mice compared with the levels in the controls, the difference being significant (Fig. 3 *C* and *D*) ($n = 4$).

TCDD Exposure in Utero Did Not Reduce the Number of Non-GABAergic Neurons in the Deeper Cortical Layers of the p27^{Kip1} Knockout Mice. To further confirm the role of p27^{Kip1} in the events associated with TCDD exposure in utero, we repeated the in utero TCDD exposure experiments using p27^{Kip1} knockout mice (p27$^{-/-}$) (Fig. 4*A*) (20–22). We have previously reported that an increased thickness of the somatosensory neocortex on P21 in p27$^{-/-}$ mice compared with that in the wild-type animals is caused by the overproduction of non-GABAergic projection neurons destined for the superficial neocortical layers (16). Here, neither the layer thickness nor the number in non-GABAergic neurons of the primary somatosensory neocortex on P21 was significantly reduced in the TCDD-treated p27$^{-/-}$ compared with the findings in the controls (i.e., p27$^{-/-}$ mice exposed to corn oil; $n = 5$) (Fig. 4 *B–D*).

Discussion

Reduction in the Peak Population Size of NPCs by TCDD Exposure. The neocortical surface area, although influenced by multiple factors such as neuropil expansion and other growth-related parameters, is mostly determined during its ontogeny by the degree of tangential expansion of PVE (9). The size of the PVE, in turn, is virtually exclusively determined by the maximum population size of the NPCs, because dominant constituents of the PVE are the NPCs (9). Thus, the reduction of the neocortical surface area in the TCDD-treated mice (Fig. 1) strongly indicates a decrease in the maximum number of NPCs during neocortical histogenesis. The population size of the NPCs is governed solely by the pattern of ascent of the Q fraction during the early phase of neocortical histogenesis, and the maximum size is reached at the

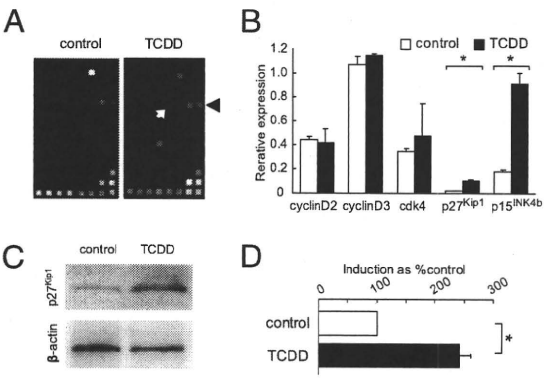

Fig. 3. Effects of in utero TCDD exposure on the expression profile of cell-cycle regulatory genes in the NPCs. (*A*) cDNA expression arrays hybridized with biotinylated probes generated from the embryonic forebrain of control and TCDD-treated mice. Black arrowhead and white arrow indicate signals from *p15*^{INK4b} and *p27*^{Kip1}, respectively. (*B*) mRNA expression after TCDD exposure. The β-actin signal equals 1.0. (*C*) Immunoblot analysis of nuclear p27^{Kip1} protein in the forebrains of the embryos of the control and TCDD-treated mice. β-actin levels were used to verify equal loading of the samples. (*D*) TCDD-induced increase of nuclear p27^{Kip1} protein. Bars, percentage signal intensity relative to the levels in the control embryos set at 100%. *$P < 0.05$. Error bars in *B* and *D*, SEM.

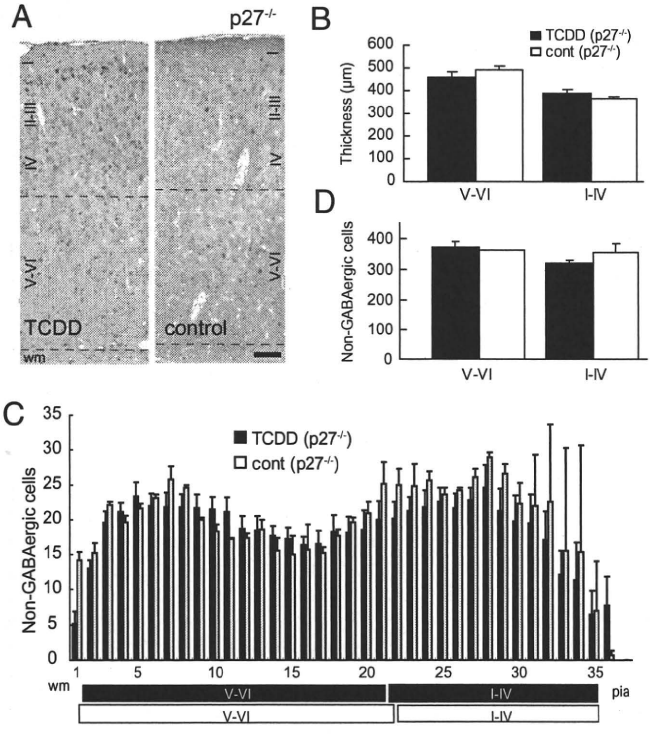

Fig. 4. Effects of in utero TCDD exposure in $p27^{Kip1}$ knockout mice as assessed on P21. (*A*) High-power view of the primary somatosensory neocortex of $p27^{Kip1}$ knockout mice ($p27^{-/-}$) exposed to TCDD and control mice. Brown cells, GABA-positive interneurons; purple nuclei, either non-GABAergic projection neurons or glial cells; black dotted lines, boundaries between layers I-IV/V-VI and gray matter/wm. (Scale bar, 100 μm.) (*B*) Thickness of layers V-VI and I-IV in the TCDD-treated and control mice shown in *A*. (*C*) Numbers of non-GABAergic neurons counted in each bin (250 μm in width and 25 μm in height) lined serially from the wm to the pia in the primary somatosensory neocortex shown in *A*. Black and white boxes under the abscissa indicate layers I-IV/V-VI in the neocortex of the TCDD-treated and control mice, respectively. (*D*) Total number of non-GABAergic neurons in layers V-VI and I-IV. Error bars in *B–D*, SEM.

point where the Q fraction reaches 0.5: the earlier the Q fraction reaches 0.5, the smaller the peak NPC population size (9, 23). Because no increase in apoptosis was noted in the PVE of the TCDD-treated mice, we conclude that TCDD exposure in utero reduced the peak population size of the NPCs by inducing a premature increase of the Q fraction. Because the degree of surface-area reduction is relatively small (7%), the premature increase in the Q fraction to 0.5 was likely to have occurred relatively late during the period, when the Q fraction was between 0 and 0.5. This assumption agrees with the previously reported $p27^{Kip1}$ expression pattern among NPCs (that is, extremely low at the outset with the peak expression in the middle of neuronogenesis) (24).

Possible Mechanisms of Underproduction of Non-GABAergic Neurons in the Deeper Cortical Layers. It is of critical importance to note that only those projection neurons that are produced during the early phase of neuronogenesis when the Q fraction is less than 0.5 become destined for the deeper cortical layers (9, 10). It follows that the time point at which the Q fraction reaches 0.5 during neuronogenesis is the critical time window for the phenotypic switch from the deep- to superficial-layer neurons (25). Taken together, we conclude that the abnormal increase of the Q fraction during the early phase of neuronogenesis induced by TCDD exposure leads not only to a decrease of the peak population size of the NPCs but also to premature-cell phenotype switch and consequently, a decrease in the number of non-GABAergic projection neurons in the deeper cortical layers.

Of note, the progenitor population of the PVE is already committed to their lineage without pluripotency. In fact, our preliminary results indicated that GABAergic neurons and glial cells were also reduced in number, and such reduction was not observed in $p27^{-/-}$. It follows that $p27^{Kip1}$ is likely to be responsible for determining the size of those neural populations as well. The proliferation/differentiation characteristics of progenitor populations of GABAergic neurons (NPCs of the ganglionic eminence) and glial cells surely deserve further investigation (26).

Mechanism of Nuclear Accumulation of $p27^{Kip1}$ After TCDD Exposure. The premature increase of the Q fraction, as described in the foregoing paragraphs, is the underlying biological mechanism for the TCDD-induced abnormality of neocortical histogenesis. The increase of the Q fraction seems to be attributable to the nuclear accumulation of $p27^{Kip1}$: this hypothesis is lent strong support by the finding that mice lacking the $p27^{Kip1}$ protein showed almost no alteration of the neocortical thickness after TCDD exposure (Fig. 4). Thus, $p27^{Kip1}$ may be involved in the cascade of critical events anywhere downstream of the direct effect of TCDD. There has been no report to this date, to the best of our knowledge, on the effect of TCDD on the subcellular localization of the $p27^{Kip1}$. The nuclear fraction of $p27^{Kip1}$ protein is determined by the balance of the protein transportation into and out of the nuclei. However, the expression levels of Jab-1, Akt, and Skp2 proteins, known to be involved in the nuclear transportation and degradation of the $p27^{Kip1}$ protein, were not found to be altered in the NPCs of the TCDD-treated mice (27–31). Another intriguing observation is the stability of the total cell-cycle length observed, despite TCDD exposure (Table 1). The stabilizing mechanisms of the cell-cycle kinetics shown in *Drosophila melanogaster* (32) may also be involved in the homeostasis of the NPC cell cycle after in utero TCDD exposure.

This report quantitatively evaluates the effects of an environmental pollutant on neocortical histogenesis. In addition, this study is an example of an experimental model where the phenotypic severity of a particular adverse effect of a given environmental substance was found to be dependent on the genotype of the animals, which has profound implications from the viewpoint of toxicogenomics (33). Furthermore, our mathematical model of neocortical histogenesis has been shown to be a powerful tool to examine neocortical dysgenesis after relatively subtle alterations in the decision-making characteristics of the NPCs. We believe that this analytical method would be applicable to various environmental substances that may have adverse effects on human CNS development.

Materials and Methods

TCDD Administration. TCDD (Cambridge Isotope Laboratory) was dissolved in corn oil at a concentration of 2 μg mL^{-1}. A single dose of TCDD solution, or corn oil {0.01 mL [gram body weight (g bw)]$^{-1}$} as control, was administered orally to pregnant C57BL/6N and $p27^{-/-}$ mice on E7 using a disposable feeding needle. The total dose of TCDD administered was 20 μg (kg bw)$^{-1}$. This dose was adopted, because it was expected not to affect the mother in terms of child-rearing behavior. In fact, no adverse effect was observed during pregnancy and the postpartum period.

Measurement of the Dimensions of the Telencephalon. Brains from either TCDD- or corn oil-exposed mice on P21 were fixed in 4% phosphate-buffered formaldehyde containing 0.5% glutaraldehyde by transcardiac perfusion. The length and width of 10 telencephalons obtained from either TCDD- or corn oil-exposed P21 mice embryos were measured with micrometer calipers.

GABA Immunohistochemistry, Cumulative BrdU Labeling Analysis, and Q Fraction Analysis. GABA immunohistochemistry was performed as described previously using anti-GABA antibody (Chemicon International) (16). Cumulative BrdU labeling analysis (18) and Q fraction analysis (9, 15, 34) were performed as previously described. Detailed methods are described in *SI Materials and Methods*.

mRNA Expression Analysis and Immunoblot Analysis. Total RNA was isolated from E12 cerebral walls using the RNeasy Protect kit (Qiagen), and the mRNA was purified using the MicroPolyA Pure kit (Ambion) for generating biotinylated cDNA probes. The biotinylated probes were hybridized to cDNA expression arrays (GE array Q series Mouse Cell Cycle Gene Array; Superarray). Immunoblot analyses were conducted using anti-$p27^{Kip1}$, $p15^{INK4b}$, cyclin E, Skp2, β-actin (Santa Cruz Biotechnology), cyclin D1, CDK2, CDK4 (Sigma), AKT (Cell Signaling Technology), and Jab-1 (GeneTex) antibodies. Detailed methods are described in *SI Materials and Methods*.

ACKNOWLEDGMENTS. $p27^{Kip1}$ knockout mice were provided by Nippon Roche K.K. which were generated by Nakayama K, et al. (20). We acknowledge the assistance of Ms. H. Zaha and the discussions that we held with Drs. C. Tohyama and T. Goto during the preparation of this manuscript. This work was supported by Grant-in-Aid for Young Scientists (B) of the Ministry of Education, Culture, Sports, Science and Technology of Japan (17790723, 20790744, and 22791001 to T.M.) and Grant-in-Aid for Scientific Research (B) of Japan Society for the Promotion of Science (JSPS) (15390327, 18390302, and 20390299 to T.T.) and the 21st century Center of Excellence program of JSPS.

1. Barsotti DA, Abrahamson LJ, Allen JR (1979) Hormonal alterations in female rhesus monkeys fed a diet containing 2,3,7,8-tetrachlorodibenzo-p-dioxin. *Bull Environ Contam Toxicol* 21:463–469.
2. Birnbaum LS (1994) Endocrine effects of prenatal exposure to PCBs, dioxins, and other xenobiotics: Implications for policy and future research. *Environ Health Perspect* 102: 676–679.
3. Poland A, Knutson JC (1982) 2,3,7,8-tetrachlorodibenzo-p-dioxin and related halogenated aromatic hydrocarbons: Examination of the mechanism of toxicity. *Annu Rev Pharmacol Toxicol* 22:517–554.
4. Markowski VP, Cox C, Preston R, Weiss B (2002) Impaired cued delayed alternation behavior in adult rat offspring following exposure to 2,3,7,8-tetrachlorodibenzo-p-dioxin on gestation day 15. *Neurotoxicol Teratol* 24:209–218.
5. Chen YC, Guo YL, Hsu CC, Rogan WJ (1992) Cognitive development of Yu-Cheng ("oil disease") children prenatally exposed to heat-degraded PCBs. *JAMA* 268:3213–3218.
6. Perera FP, et al. (2009) Prenatal airborne polycyclic aromatic hydrocarbon exposure and child IQ at age 5 years. *Pediatrics* 124:e195–e202.
7. Sauer FC (1935) Mitosis in the neural tube. *J Comp Neurol* 62:377–405.
8. Takahashi T, Nowakowski RS, Caviness VS, Jr (1995) The cell cycle of the pseudostratified ventricular epithelium of the embryonic murine cerebral wall. *J Neurosci* 15:6046–6057.
9. Takahashi T, Nowakowski RS, Caviness VS, Jr (1996) The leaving or Q fraction of the murine cerebral proliferative epithelium: a general model of neocortical neuronogenesis. *J Neurosci* 16:6183–6196.
10. Takahashi T, Goto T, Miyama S, Nowakowski RS, Caviness VS, Jr (1999) Sequence of neuron origin and neocortical laminar fate: Relation to cell cycle of origin in the developing murine cerebral wall. *J Neurosci* 19:10357–10371.
11. Sherr CJ, Roberts JM (1999) CDK inhibitors: Positive and negative regulators of G1-phase progression. *Genes Dev* 13:1501–1512.
12. Toyoshima H, Hunter T (1994) p27, a novel inhibitor of G1 cyclin-Cdk protein kinase activity, is related to p21. *Cell* 78:67–74.
13. Polyak K, et al. (1994) Cloning of p27Kip1, a cyclin-dependent kinase inhibitor and a potential mediator of extracellular antimitogenic signals. *Cell* 78:59–66.
14. Mitsuhashi T, et al. (2001) Overexpression of p27Kip1 lengthens the G1 phase in a mouse model that targets inducible gene expression to central nervous system progenitor cells. *Proc Natl Acad Sci USA* 98:6435–6440.
15. Tarui T, et al. (2005) Overexpression of p27 Kip 1, probability of cell cycle exit, and laminar destination of neocortical neurons. *Cereb Cortex* 15:1343–1355.
16. Goto T, Mitsuhashi T, Takahashi T (2004) Altered patterns of neuron production in the p27 knockout mouse. *Dev Neurosci* 26:208–217.
17. Kolluri SK, Weiss C, Koff A, Göttlicher M (1999) p27(Kip1) induction and inhibition of proliferation by the intracellular Ah receptor in developing thymus and hepatoma cells. *Genes Dev* 13:1742–1753.
18. Takahashi T, Nowakowski RS, Caviness VS, Jr (1992) BUdR as an S-phase marker for quantitative studies of cytokinetic behaviour in the murine cerebral ventricular zone. *J Neurocytol* 21:185–197.
19. Nowakowski RS, Lewin SB, Miller MW (1989) Bromodeoxyuridine immunohistochemical determination of the lengths of the cell cycle and the DNA-synthetic phase for an anatomically defined population. *J Neurocytol* 18:311–318.
20. Nakayama K, et al. (1996) Mice lacking p27(Kip1) display increased body size, multiple organ hyperplasia, retinal dysplasia, and pituitary tumors. *Cell* 85:707–720.
21. Kiyokawa H, et al. (1996) Enhanced growth of mice lacking the cyclin-dependent kinase inhibitor function of p27(Kip1). *Cell* 85:721–732.
22. Fero ML, et al. (1996) A syndrome of multiorgan hyperplasia with features of gigantism, tumorigenesis, and female sterility in p27(Kip1)-deficient mice. *Cell* 85: 733–744.
23. Takahashi T, Nowakowski RS, Caviness VS, Jr (1997) The mathematics of neocortical neuronogenesis. *Dev Neurosci* 19:17–22.
24. Delalle I, Takahashi T, Nowakowski RS, Tsai LH, Caviness VS, Jr (1999) Cyclin E-p27 opposition and regulation of the G1 phase of the cell cycle in the murine neocortical PVE: A quantitative analysis of mRNA in situ hybridization. *Cereb Cortex* 9:824–832.
25. Caviness VS, Jr, et al. (2003) Cell output, cell cycle duration and neuronal specification: A model of integrated mechanisms of the neocortical proliferative process. *Cereb Cortex* 13:592–598.
26. Bhide PG (1996) Cell cycle kinetics in the embryonic mouse corpus striatum. *J Comp Neurol* 374:506–522.
27. Tomoda K, et al. (2002) The cytoplasmic shuttling and subsequent degradation of p27Kip1 mediated by Jab1/CSN5 and the COP9 signalosome complex. *J Biol Chem* 277: 2302–2310.
28. Kossatz U, et al. (2004) Skp2-dependent degradation of p27kip1 is essential for cell cycle progression. *Genes Dev* 18:2602–2607.
29. Carrano AC, Eytan E, Hershko A, Pagano M (1999) SKP2 is required for ubiquitin-mediated degradation of the CDK inhibitor p27. *Nat Cell Biol* 1:193–199.
30. Nakayama K, et al. (2000) Targeted disruption of Skp2 results in accumulation of cyclin E and p27(Kip1), polyploidy and centrosome overduplication. *EMBO J* 19:2069–2081.
31. Liang J, et al. (2002) PKB/Akt phosphorylates p27, impairs nuclear import of p27 and opposes p27-mediated G1 arrest. *Nat Med* 8:1153–1160.
32. Reis T, Edgar BA (2004) Negative regulation of dE2F1 by cyclin-dependent kinases controls cell cycle timing. *Cell* 117:253–264.
33. Shih DM, et al. (1998) Mice lacking serum paraoxonase are susceptible to organophosphate toxicity and atherosclerosis. *Nature* 394:284–287.
34. Hayes NL, Nowakowski RS (2000) Exploiting the dynamics of S-phase tracers in developing brain: Interkinetic nuclear migration for cells entering versus leaving the S-phase. *Dev Neurosci* 22:44–55.

Chapter 13

Oxidative Stress-Mediated Signaling Pathways by Environmental Stressors

Hideko Sone and Hiromi Akanuma*

National Institute for Environmental Studies, Tsukuba, Ibaraki, Japan.
**Email: hsone@nies.go.jp*

13.1 INTRODUCTION

Oxidative stress in the form of excess reactive oxygen species (ROS) or reactive nitrogen species (RNS) can affect cells deleteriously or beneficially. Such stress might be generated by intracellular or extracellular sources. Furthermore, oxidative stress can cause various biological effects. Environmental stress is a key contributor to human disease. a number of substances such as metals, particulate materials, smoke, pesticides, and physical agents are environmental stressors [1] that contribute to many diseases. Concerns related to environmental stressor-related diseases such as cancer, chronic lung

Oxidative Stress in Vertebrates and Invertebrates: Molecular Aspects of Oxidative Stress on Cell Signaling.
Edited by Tahira Farooqui and Akhlaq A. Farooqui

disease, diabetes mellitus, neurodegenerative diseases, and reproductive disorders have been raised recently. Research efforts elucidating the modes by which environmental stressors influence the development and progression of diseases or exploring preventive approaches are expected to engender further improvements in our knowledge. Understanding environmental stressor-induced influences at the molecular level will also provide a wealth of information related to the exploration of biomarkers for environmental stressor-related diseases [2-4].

The mechanisms of redox adaptation in living bodies and cells might involve multiple influences on an active redox-sensitive signaling pathway, such as ROS metabolism and antioxidant defenses, p53 pathway signaling, nitric oxide (NO) signaling pathway, hypoxia signaling, transforming growth factor (TGF) β-bone morphogenetic protein (BMP) signaling, tumor necrosis factor (TNF) ligand-receptor signaling, and mitochondrial function (Table 13.1). For example, transcription factors such as nuclear factor-κB (NF-κB), Nuclear factor erythroid 2-related factor 2 (Nrf2), c-Jun and hypoxia-inducible factor-1 (HIF-1) engender increased expression of anti-oxidant molecules such as superoxide dismutase (SOD), catalase, thioredoxin, and the GSH antioxidant system. Metal ions such as arsenic (III /V) or copper (II) directly influence expression levels of those transcription factors and induce various oxidative stress events including thiol molecule perturbation, generation of oxidative DNA adducts, and induction of oxidative molecular biomarkers [5-8]. Non-metal chemicals such as retinoic acids and 2,3,7,8-tetrachlorodibenzo-*p*-dioxin (TCDD) are also known to influence the expression of oxidative stress-related genes and proteins during carcinogenesis and during embryonic

development [9-12]. In relation to cancer, a growing tumor might also produce intracellular and extracellular oxidative stress, which can modify its malignant features. Endogenous sources of tumor ROS or RNS include impaired intracellular genomes or proteomes, metabolism pathways, and xenobiotic metabolism. Consequently, the study of transcriptional regulation of gene expression in the research field of oxidative stress has been useful for identifying new trans-regulatory factors or new biomarkers induced by exposure to environmental stressors.

Microarray technology has been used in environmental toxicology and biology studies and has led to the establishment of gene expression signatures profiling the toxicity of environmental stressors [13-14]. Statistical methods used for DNA microarray studies are mostly multivariate approaches. Although basic methods treat genes as traits, which are consistent with the rules of experimental design, several approaches have been developed using expression ratio datasets. Such approaches regard the genes as cases and the array plates as variables. Most well known methods based on singular value decomposition have used principal component analysis [15-16]. In alternative approaches, our previous reports have described that a Bayesian network technique, which is a probabilistic graphical model that represents a set of variable identities, is applicable to investigation of the gene expression interaction networks and the detection of differences arising in them from exposure to different doses of chemicals [17-18]. Bayesian network techniques can provide predictive information related to the relations between agents and gene expression signatures in life science fields [19-21].

This chapter addresses various environmental stressor-induced toxicities in experimental animals like rats and humans to elucidate the molecular mechanisms underlying toxicity-induced oxidative stress.

13.2 OXIDATIVE STRESS MEDIATED SIGNALING PATHWAYS

Cells respond and adapt to environmental signals such as stressors [22-24] through multiple mechanisms that involve communication pathways and signal transduction processes. The impact of oxidative stress on various diseases and aging has been reviewed comprehensively. In particular, free-radical-induced oxidative stress plays an important role in cancer development, metabolic related diseases like diabetes and hypertentions, and neurodegenerative disorders [4, 25-36]. Our survey of microarray databases and many other published references has revealed the categorical pathways induced by oxidative stress, as presented in Table 13.2.

ROS metabolism and antioxidant defenses center upon ROS, which are necessary for biological functions and which regulate many signal transduction pathways by directly reacting with and modifying the structure of proteins, transcription factors, and genes to modulate their functions. Actually, ROS induce expression levels of genes associated with signaling cell growth and differentiation, regulating the activity of enzymes (such as ribonucleotide reductase and peroxidase). Control of ROS levels is achieved by balancing ROS generation with their elimination through ROS-scavenging systems such as superoxide dismutases (SOD1, SOD2, and SOD3), glutathione

peroxidase, peroxiredoxins, glutaredoxin, and thioredoxin catalase. The ROS can modulate the activities and expression of many transcription factors and signaling and signaling proteins that are involved in stress response and cell survival through multiple mechanisms. Therefore, this category includes glutathione peroxidases (GPx), peroxiredoxins (TPx), superoxide dismutases (SOD), genes involved in superoxide metabolism such as arachidonate 12-lipoxygenase (ALOX12), and copper chaperone for superoxide dismutase (CCS). In fact, p53 signaling plays a central role in coordinating the cellular responses to a broad range of cellular stress factors; p53 functions as a node for organizing whether the cell responds to various types and levels of stress with apoptosis, cell cycle arrest, senescence, DNA repair, cell metabolism, or autophagy. Moreover, p53 controls transactivation of target genes, which is an essential feature of stress response pathways [37-39]. In other words, p53 activation leads to a complicated network of responses to the various stress signals encountered by cells [40-44]. The mitochondrial respiratory chain produces nitric oxide (NO), which can generate other reactive nitrogen species (RNS) when cells are under hypoxic conditions. Although excess ROS and RNS can engender oxidative and nitrosative stress, moderate-to-low levels of both function in cellular signaling pathways. Especially important are the roles of these mitochondria-generated free radicals in hypoxic signaling pathways, which have important implications for cancer, inflammation, and various other diseases [25, 45]. Hypoxic signaling events include vasodilation, modulation of mitochondrial respiration, and cytoprotection following ischemic insult. These phenomena are attributed to the reduction of nitrite anions to nitric oxide if local oxygen levels in tissues decrease [46],

which activates the expression of genes through oxygen-sensitive transcription factors including HIF and NF-κB. Hypoxia-dependent gene expression can have important physiologic or pathophysiologic consequences for an organism, depending upon the cause of the hypoxic insult [47]. These NO signaling and hypoxia signaling pathways are linked to the p53 pathway [48], because recent studies have shown that HIF2alpha inhibition promotes p53-mediated responses by disrupting cellular redox homeostasis, thereby permitting ROS accumulation and DNA damage [49]. Reportedly, hypoxia activates the tumor suppressor protein p53 by up-regulating Sema3E expression [50].

TGF-β-BMP signaling is involved in developmental morphogenesis and cancer morphogenesis. Morphogens such as those of the TGF-β family inhibit and stimulate basic cell proliferation, respectively, at high and low concentrations. A signaling gradient of declining TGF-β concentration regulates the inhibition and stimulation of cell proliferation [51]. Reactive oxygen species (ROS) can activate TGF-β either directly or indirectly via the activation of proteases. In addition, TGF-β itself induces ROS production as part of its signal-transduction pathway. Pulmonary tissues are vulnerable to the toxic effects of inhaled air. The oxidant pathways are especially relevant in the lung, where TGF-β is known to have a role in tissue repair and connective tissue turnover. In pulmonary fibrosis and renal endothelial cells, TGF-β activation is considered as a hallmark of disease progression [52-53]. In ovarian cancer, over-expression of FOXG1 contributes to TGF-β resistance through inhibition of p21WAF1/CIP1 expression, which is repressed by p53 [54]. Recent studies have revealed some additional novel functions of the p53 pathway. These include the down-regulation of two central cell-growth pathways,

the IGF/AKT-1 and mTOR pathways, and the up-regulation of the activities of the endosomal compartment [55-57]. The mTOR pathway including the IGF-1/AKT pathway plays critical roles in regulation of cell proliferation, survival, and energy metabolism to shut down cell growth and division to avoid the introduction of infidelity in to the process og cell growth and division [58-59]. In response to stress, IGF-BP3, PTEN, TSC2, AMPK beta1, and Sestrin1/2 are transcribed by p53 and play a critical role as negative regulators and leads to the reduction in the activities of these two pathways. Furthermore, p53 transcriptionally regulates TSAP6, Chmp4C, Caveolin-1, and DRAM, which are critical genes in the endosomal compartment, and increases exosome secretion and increases exosome secretion, the rate of endosomal removal of growth factor receptors from cell surface, and enhances autophagy [60-63]. It is thought that p53-mediated these activities lead to slow down cell growth and division, conserve and recycle cellular resources, communicate with adjacent cells and dendritic cells of the immune system, and inform other tissues of the stress signals [55, 64-65].

Tumor necrosis factor (TNF) ligand–receptor signaling occurs because TNF, as a multifunctional cytokine, can induce cell death through receptor-mediated caspase activation and mitochondrial dysfunction by a trigger of oxidative stress induced in cardiovascular disease, neuronal disease, and cancer [66]. Opposing these cell death-promoting signals, binding of TNF receptors can also trigger survival signal activation. A critical balance among various intracellular signaling pathways determines the predominant *in vivo* bioactivity of TNF, as best exemplified by the differential responses of various organs.

A major source of ROS in cells is the mitochondria. Electron leakage from the mitochondrial respiratory chain can react with molecular oxygen, resulting in the formation of the superoxide anion radical, which can subsequently be converted to other ROS. In phagocytes and some cancer cells, ROS are producible through a reaction that is catalyzed by NADPH oxidase complexes. When attackers from the outside, as environmental stressors, damage mitochondria, electron leakage is also induced; this dysfunction induces severe problems in tissues [67-70]. Mitochondrial dysfunction causes the onset of some diseases [71-74]. Recent evidence has shown that mitochondrial dysfunction is related closely to insulin resistance and metabolic syndrome. The underlying mechanism of mitochondrial dysfunction is very complex, including genetic factors from both the nucleus and mitochondrial genome, with numerous environmental factors also impacting [75].

Exposure to air pollution, including particles, metals, and other organic compounds as environmental stressors, is associated with pulmonary diseases and cancer. The mechanisms of induced health effects are believed to involve oxidative stress. Oxidative stress mediated by airborne particles and/or fibers might arise from direct generation of ROS from the surfaces of particles and fibers, soluble compounds such as transition metals or organic compounds, and activation of inflammatory cells capable of generating ROS and RNS. Generation of ROS/RNS can cause covalent modifications to DNA directly or they can initiate the formation of genotoxic lipid hydroperoxides. The resulting oxidative DNA damage can engender changed gene expression such as upregulation of tumor promoters and downregulation of tumor suppressor genes; the

DNA damage might therefore be implicated in cancer development. This chapter describes the important role of free radicals in particle- and fiber-induced cellular damage, the interaction of ROS with target molecules, especially with DNA, and the modulation of specific genes and transcription factor caused by oxidative stress. Consequently, various environmental stressors cause cellular damage through oxidative stress induction and many signaling pathways. However, what environmental stressor is dominant in which signaling pathway is not always clear. Therefore, identifying gene expression signatures extracted from microarray data can clarify how environmental stressors may damage cells and engender diseases.

13.2.1 Case studies in tissues or organs from rats exposed to environmental stressors

Many animal models have been studies to elucidate mechanisms of action of oxidants or antioxidant. Oxidative stress and its defense research have expanded dramatically due to its potential benefit in disease prevention and health promotion. Especially, the experiments using rats exposed to stress-induced chemicals been extensively studied in biological systems such as cell cultures, animal models and clinical trials [76-79]. Therefore, 33 independent studies in rats were focused in this chapter because these studies used microarray in where gene expression data are publicly available from the Gene Expression Omnibus (GEO; http://www.ncbi.nlm.nih.gov/gds). These microarray data with the same platform GPL341 (Affymetrix) sets in rats were

downloaded for this study. All datasets were normalized across all arrays using *Z*-score transformation methods after combination with respect to probe IDs. The normalized values were filtered with oxidative-related genes listed in this work (Table 13.2) and then the top 10 genes from up-regulated and down-regulated genes were chosen to analyze gene expression signatures (Table 13.3). The selected genes were classified using principal component analysis to create gene expression signatures of oxidative stress, and were divided into six groups. Most selected genes could be assigned to gene ontology (GO) categories: DNA repair, oxygen and reactive oxygen species metabolism, and response to stress, but cyclins and cyclin dependent kinase contained in "Apoptosis related genes, Cell Cycle Arrest and Checkpoint, Regulation of the Cell Cycle, Regulation of Cell Proliferation, Cell Growth and Differentiation" of "p53 signaling" and "TGF-beta signaling" were not observed. Experimental conditions selected from GPL341 datasets in this work were almost all of short-period exposure using *in vivo* and *in vitro* culture systems of rats. It is noteworthy that microarrays capture only transient responses to oxidative stimuli. However, we can predict the underlying mechanism of environmental stressors through oxidative signatures for gene expression. For example, mehtylprednisolone [80, 81], streptozotocin[82], trimethyltin [83], and octreotide [84] up-regulate GPXs, NOS, and NOX, suggesting that environmental stessors in the cluster 1 can activate the NO signaling that leads inflammation or other cellular damage . Thioredoxin interacting protein, Txnip, was identified as a unique gene in this category. In cluster 2 (GDS696 [85],GDS880 [86], GDS1518 [87], GDS1626 [88], GDS2107 [89], GDS2372 [90], GDS2457 [91], GDS2688 [92]), Rad23, Rad50, Rad51c, which are DNA

repair and recombination proteins, and the other DNA replication proteins DNA-directed DNA polymerase delta (Pold)1 and Pold3 were classified. This classification suggests that environmental stressors in cluster 2 such as fibronectin, protein restriction, heregulin, kainic acid, hypoxia and ethanol harmed mitochondria or damaged DNA more than the stressors in cluster 1. In cluster 3 (GDS1363 [93], GDS1452[94], GDS1922 [95], GDS2037 [96], GDS2073 [97], GDS2093 [98], GDS 2194 [99], GDS2616 [100], GDS2639 [101], GDS2774 [102], GDS2901 [103], GDM1038 [104]), Gadd45a, Nthl1, Mgmt, Mpp4, Chek1 Cry2, Txnrd1 were observed as up-regulated genes. Since these genes interact with DNA repair and p53 signaling activated, it is possible that environmental stressors in the cluster 3 cause DNA damage and remodeling. In cluster 4 (GDS902 [105], GDS2243 [106], GDS2361 [107]), DNA replication proteins Pinx1 and Slk were detected as unique genes. Especially, STE20-like kinase (Slk) appears to influence cell survival and proliferation. In fact, Slk has been suggested to have a central growth-suppressive role for Mst orthologs, with intriguing possible links to other established tumor suppressors through work in model organisms. A part of genes in cluster 5 (GDS1027 [108], GDS1273 [109], GDS1959 [110]) was overlaped in clusters 1 and 3. In cluster 6 (GDS1354 [111], GDS2231 [112]), a part of genes was overlaped in clusters 2 and 4. However, Vim was detected as a unique gene in GDS1354, which is an experiment in cirrhotic rats [111] since up-regulation of this gene was also observed in renal cell carcinoma [113], cerebral tumors [114], germ cells, and trophoblastic neoplasms [115].

13.2.2 Prediction of biological influences from gene expression signatures in rats exposed to environmental stressors

These clusters were characterized by several biological functions. Data of gene expression signatures in Table 13.3 were analyzed through the use of Ingenuity Pathways Analysis (Ingenuity® Systems, www.ingenuity.com). The Functional Analysis identified the biological functions that were most significant to the data set. Molecules from the dataset that met the expression value were associated with biological functions and/or diseases in Ingenuity's Knowledge Base were considered for the analysis. Right-tailed Fisher's exact test was used to calculate a *P*-value determining the probability that each biological function and/or disease assigned to that data set is due to chance alone. In Table 13.4, the highest probability predictive function in the cluster 1 showed "DNA Replication, Recombination, and Repair"; it in the cluster 2 showed "Small Molecule Biochemistry"; it in the cluster 3 also showed "Small Molecule Biochemistry"; it in the cluster 4 showed "DNA Replication, Recombination, and Repair"; it in the cluster 5 showed "Cancer"; it in the cluster 6 showed "Lipid Metabolism". In "Small Molecule Biochemistry", genes related with "degradation or catabolism of hydrogen peroxide" like CAT, GPX3 and GPX4 and peroxidation of lipid were affected in cluster 2, 3 and 6. In "Gene expression", genes related with "binding of p53 consensus binding site" like APEX1, BRCA1 and PTTG1 were affected. For instance, the top-rated network generated by retinoic X receptor ligand LG100268 was showed in Figure 13.1. This

network consists of a cluster of 16 molecules meet 44 molecules, which are belong to biological functions of DNA replication, recombination and repair, cancer and cell cycle.

13.2.3 Oxidative stress-mediated p53 pathways in human tissues

Among many oxidative responsive pathways, p53 signaling has been studied extensively and has been thought to play a main role in the orchestration of oxidative events in cells. It coordinates the cellular responses to a broad range of cellular stress factors. In fact, p53 functions as a node for organizing whether the cell responds to various types and levels of stress with apoptosis, cell cycle arrest, senescence, DNA repair, cell metabolism, or autophagy, as described earlier in this chapter [37-39]. To control and fine-tune responses to various stress signals encountered by cells, as a transcription factor that both activates and represses a broad range of target genes, p53 demands an exquisitely complicated regulatory network (Figure 13.2). The classical model for activation of p53 specifically examines three simple and rate-limiting steps: p53 stabilization induced by ataxia telangiectasia mutated (ATM) / ataxia telangiectasia and Rad3 related (ATR)-mediated phosphorylation, sequence-specific DNA binding, and target gene activation through interaction with the general transcriptional machinery [29]. Recent studies with animal models describe that mouse double minute (Mdm) 2 and MdmX might determine whether a cell responds to p53 activation with growth arrest or apoptosis, but the molecular mechanism of these differential effects remains unknown. In fact, Mdm2 and MdmX can both be recruited to p53 promoter regions. Via a multitude of

mechanisms, they can repress transcription of p53 target genes [116-118]. The p53 protein binds sequence-specific regions of DNA of the target gene to process sensing and removal of oxidative damage to nuclear DNA and genetic instability. Furthermore, p53 acts as a transcription factor to regulate the expression of many pro-oxidant and antioxidant genes. A new refined model for p53 activation includes three key steps: (1) p53 stabilization, (2) anti-repression, and (3) promoter-specific activation. Among the three steps, most environmental stressors contribute mainly to p53 stabilization and promoter-specific activation. Several reports describe that small weight molecules engender induction of stress-induced genes such as NAD(P)H dehydrogenase, quinone (NQO)1 and NQO2, which stabilize and transiently activate p53 and downstream genes leading to protection against adverse effects of stressors [119-121] .

Therefore, to understand how stress-induced genes are downstream within the p53 pathway, we analyzed gene expression of p53 signaling pathways in array datasets GDS2780 [122] and GSE7967 [123] that had been obtained from the GEO database. In the GDS2780 study, six heavy metals and three organic compounds that were exposed in liver carcinoma HepG2 cells responded dramatically to gene expression of CHK1, CHK2, Cyclin B Cdc2 p21, p53R2, Cop1-1, and Gadd45 [1]. Interestingly, expression levels of p53R2 and Gadd45 responded differently to the heavy metals: p53R2 is likely to associate with mitochondrial DNA and play a critical role in embryogenesis and neurogenesis [124-128]; in contrast, Gadd45 plays a vital role as a cellular stress sensor in the modulation of cell signal transduction in response to stress. Increasing Gadd45 can stabilize p53 activation, leading to cell cycle arrest or procession to apoptosis [129-131].